Molecular Analysis of Cellulose Biosynthesis in *Arabidopsis*

Tony Arioli, *et al.*

Science **279**, 717 (1998);
DOI: 10.1126/science.279.5351.717

and *S. pombe*. Those results are consistent with a model in which iron depletion of normal hepatocytes causes increased transcription of Cp that interacts with an iron transporter (also up-regulated by iron depletion), resulting in increased iron influx. The iron depletion requirement for Cp-stimulated Fe uptake, and the inhibition by cycloheximide, are consistent with a requirement for an inducible iron transporter. Taken together, the experiments in yeast and hepatic cells demonstrate a remarkable evolutionary conservation of the mechanisms that underlie the pathway controlling eukaryotic iron metabolism by copper. However, there are noteworthy differences: in yeast, the Cp homolog is a membrane protein that is co-transported to the cell surface and is in continuous contact with the iron transporter, whereas in mammalian tissues Cp is a secreted protein, and any interaction with a transporter is likely to be transient. This difference may be related to paracrine requirements for Cp in multicellular organisms.

REFERENCES AND NOTES

1. B. R. Bacon, G. M. Brittenham, C. H. Park, A. S. Tavill, *Ann. N.Y. Acad. Sci.* **526**, 155 (1988).
2. R. S. Britton, A. S. Tavill, B. R. Bacon, in *Iron Metabolism in Health & Disease*, J. H. Brock, J. W. Halliday, M. J. Pippard, L. W. Powell, Eds. (Saunders, London, 1994), pp. 311–351.
3. J. H. Brock, in *ibid.*, pp. 353–389.
4. R. D. Klausner, T. A. Rouault, J. B. Harford, *Cell* **72**, 19 (1993).
5. L. Rydén, in *Copper Proteins and Copper Enzymes*, R. Lontie, Ed. (CRC Press, Boca Raton, FL, 1984), vol. III, pp. 37–100.
6. E. B. Hart, H. Steenbock, J. Waddell, C. A. Elvehjem, *J. Biol. Chem.* **77**, 797 (1928).
7. H. A. Ragan, S. Nacht, G. R. Lee, C. R. Bishop, G. E. Cartwright, *Am. J. Physiol.* **217**, 1320 (1969).
8. S. Osaki and D. A. Johnson, *J. Biol. Chem.* **244**, 5757 (1969).
9. _____, E. Frieden, *ibid.* **241**, 2746 (1966).
10. _____, *ibid.* **246**, 3018 (1971).
11. J. I. Logan, K. B. Harveyson, G. B. Wisdom, A. E. Hughes, G. P. R. Archbold, *Q. J. Med.* **87**, 663 (1994).
12. Z. L. Harris *et al.*, *Proc. Natl. Acad. Sci. U.S.A.* **92**, 2539 (1995).
13. H. Morita *et al.*, *Ann. Neurol.* **37**, 646 (1995).
14. D. S. Yuan *et al.*, *Proc. Natl. Acad. Sci. U.S.A.* **92**, 2632 (1995).
15. J. Kaplan and T. V. O'Halloran, *Science* **271**, 1510 (1996).
16. J. Kaplan, *J. Clin. Invest.* **98**, 3 (1996).
17. C. Askwith *et al.*, *Cell* **76**, 403 (1994).
18. D. M. De Silva, C. C. Askwith, D. Eide, J. Kaplan, *J. Biol. Chem.* **270**, 1098 (1995).
19. C. Askwith and J. Kaplan, *ibid.* **272**, 401 (1997).
20. J. G. Parkes, E. W. Randell, N. F. Olivieri, D. M. Templeton, *Biochim. Biophys. Acta* **1243**, 373 (1995).
21. H. P. Roeser, G. R. Lee, S. Nacht, G. E. Cartwright, *J. Clin. Invest.* **49**, 2408 (1970).
22. C. K. Mukhopadhyay, Z. K. Attieh, P. L. Fox, unpublished data.
23. M. E. Bouma, E. Rogier, N. Verthier, C. LaBarre, G. Feldmann, *In Vitro Cell. Dev. Biol.* **25**, 267 (1989).
24. S. White, K. Miller, C. Hopkins, I. S. Trowbridge, *Biochim. Biophys. Acta* **1136**, 28 (1992).
25. B. S. Stein and H. H. Sussman, *J. Biol. Chem.* **261**, 10319 (1986).
26. R. Stearman, D. S. Yuan, Y. Yamaguchi-Iwai, R. D. Klausner, A. Dancis, *Science* **271**, 1552 (1996).
27. B. B. Knowles, C. C. Howe, D. P. Aden, *ibid.* **209**, 497 (1980).
28. R. G. Batey, P. Lai Chung Fong, S. Shamir, S. Sherlock, *Dig. Dis. Sci.* **25**, 340 (1980).
29. C. Hershko, G. Graham, G. W. Bates, E. A. Rachmilewitz, *Br. J. Haematol.* **40**, 255 (1978).
30. For measurement of iron release, cells were preloaded with iron by incubation with 100 μM ^{55}Fe-NTA for 4 hours. The cells were washed with saline-EDTA and incubated with Cp for 30 min in RPMI medium; the amount of ^{55}Fe released into the conditioned medium was measured by liquid scintillation counting.
31. For measurement of iron uptake, cells were washed with phosphate-buffered saline and then with iron-free RPMI medium. Cells were incubated with purified human Cp (Calbiochem, San Diego, CA) in the presence of 0.5 μM ^{55}Fe-NTA and 1 mM ascorbic acid in RPMI medium for 15 min at 25°C. The cultures were washed with saline-EDTA, and the cells were harvested with NaOH; after neutralization, cellular ^{55}Fe was measured by liquid scintillation counting.
32. W. Breuer, S. Epsztejn, Z. I. Cabantchik, *J. Biol. Chem.* **270**, 24209 (1995).
33. Isolated nuclei from 5×10^7 HepG2 cells were incubated with [α-^{32}P]uridine triphosphate (100 μCi, 3000 mCi/mmol). The purified reaction products were hybridized to linearized plasmid DNAs [Cp, 15 μg of pcDNA3-Cp; vector control, 15 μg of pcDNA3; and 1 μg of pcDNA3–glyceraldehyde phosphate dehydrogenase (GAPDH)] immobilized onto a nylon membrane.

34. We are grateful to J. Gitlin (Washington University) for the full-length Cp cDNA and for helpful discussions. This work was supported by NIH grants HL29582 and HL52692 (P.L.F.) and by a Fellowship Award from the American Heart Association, Northeast Ohio Affiliate (C.K.M.).

26 August 1997; accepted 20 November 1997

Molecular Analysis of Cellulose Biosynthesis in *Arabidopsis*

Tony Arioli, Liangcai Peng, Andreas S. Betzner, Joanne Burn, Werner Wittke, Werner Herth, Christine Camilleri, Herman Höfte, Jacek Plazinski, Rosemary Birch, Ann Cork, Julie Glover, John Redmond, Richard E. Williamson*

Cellulose, an abundant, crystalline polysaccharide, is central to plant morphogenesis and to many industries. Chemical and ultrastructural analyses together with map-based cloning indicate that the *RSW1* locus of *Arabidopsis* encodes the catalytic subunit of cellulose synthase. The cloned gene complements the *rsw1* mutant whose temperature-sensitive allele is changed in one amino acid. The mutant allele causes a specific reduction in cellulose synthesis, accumulation of noncrystalline β-1,4-glucan, disassembly of cellulose synthase, and widespread morphological abnormalities. Microfibril crystallization may require proper assembly of the *RSW1* gene product into synthase complexes whereas glucan biosynthesis per se does not.

Cellulose, a crystalline β-1,4-glucan, is the world's most abundant biopolymer. Its biomass makes it a global carbon sink and renewable energy source, and its crystallinity provides mechanical properties central to plant morphogenesis and the fiber industries. The mechanisms that plants use in synthesis have not yielded to biochemistry or cloning by hybridization to genes encoding prokaryotic cellulose synthases (*1*). By combining chemical and ultrastructural analyses with map-based cloning, we show that the *Arabidopsis RSW1* locus encodes a glycosyl transferase that complements the *rsw1* mutant (*2*). The temperature-sensitive *rsw1* allele disassembles cellulose synthase complexes in the plasma membrane ("rosettes"), alters cellulose crystallinity, and disrupts morphogenesis. The gene product, which is closely related to the putative cellulose synthase catalytic subunit from cotton fibers (*3*), can therefore be used to manipulate the production and physical properties of cellulose, while the mutant links plant morphogenesis and cellulose production.

Mutants impaired in cellulose production were selected with the use of a radial swelling phenotype (*rsw*), which mimics responses of wild-type roots to cellulose synthesis inhibitors such as dichlorobenzoni-

T. Arioli, J. Burn, R. Birch, J. Glover, Cooperative Research Centre for Plant Science, Australian National University, Post Office Box 475, Canberra, ACT 2601, Australia.
L. Peng, J. Plazinski, A. Cork, J. Redmond, R. E. Williamson, Glycobiology Unit, Plant Cell Biology Group, and Cooperative Research Centre for Plant Science, Research School of Biological Sciences, Australian National University, Post Office Box 475, Canberra, ACT 2601, Australia.
A. S. Betzner, Groupe Limagrain Pacific, Post Office Box 475, Canberra, ACT 2601, Australia.
W. Wittke and W. Herth, Zellenlehre, Im Neuenheimer Feld 230, Ruprecht-Karls-Universität, D 69120 Heidelberg, Germany.
C. Camilleri and H. Höfte, Laboratoire de Biologie Cellulaire, Institut National de la Recherche Agronomique, Route de St-Cyr, 78026 Versailles Cedex, France.

*To whom correspondence should be addressed at Plant Cell Biology Group, Research School of Biological Sciences, Australian National University, Post Office Box 475, Canberra, ACT 2601, Australia. E-mail: richard@rsbs.anu.edu.au

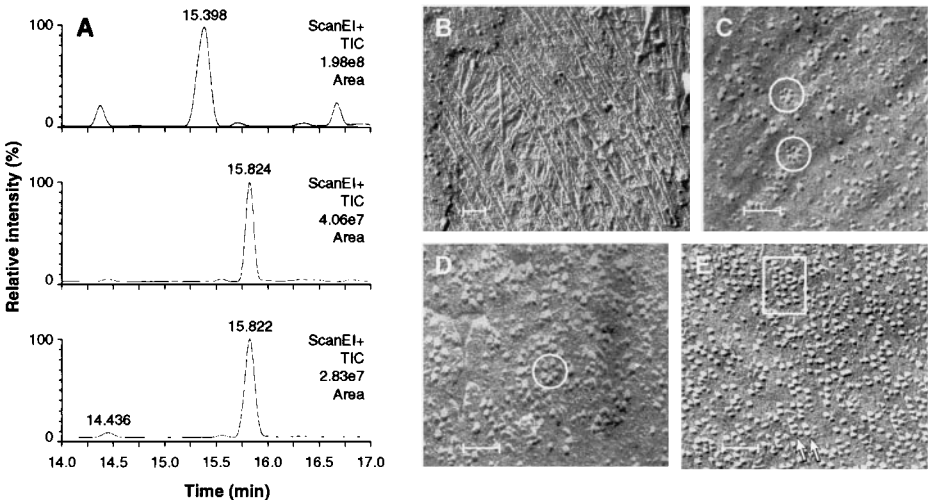

Fig. 1. (**A**) Gas chromatography of alditol acetates of methylated sugars from laminarin (top) and cellulose (middle) standards and from the glucan purified from the ammonium oxalate fraction from shoots of *rsw1* grown at 31°C (bottom). Coincident peaks show that the *rsw1* glucan is 1,4-linked. (**B** through **E**) Roots frozen in nitrogen slush without cryoprotection were freeze-fractured with the use of double replica holders in a Balzers BAF 400T (*18*). (B) Normal microfibrils in *rsw1* (18°C). (C) Rosettes (P face) of the mutant are indistinguishable from the wild type at 18°C, but (D) are rare and sometimes irregular in *rsw1* seedlings within 3 hours of transfer to 31°C. (E) Particles in rows (arrows) can curve or cluster (box) under longer (18-hour) exposures. Scale bars, 50 nm.

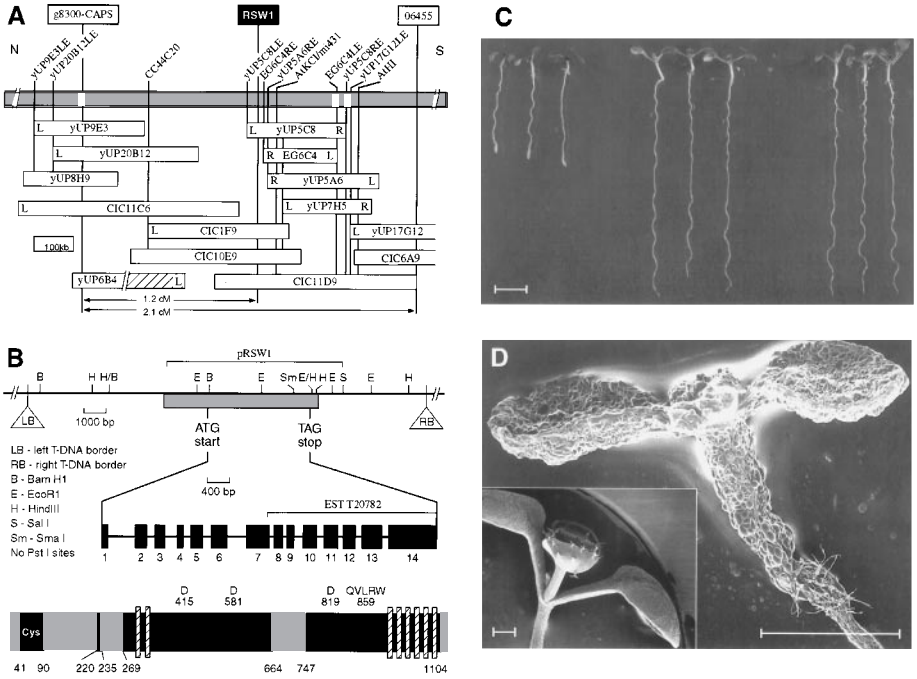

Fig. 2. (**A**) Part of contig IV from *Arabidopsis* chromosome 4 (*19*) refined with the use of primers based on partially sequenced left (L) and right (R) ends to establish YAC overlap by PCR (vertical lines), by converting g8300 to a cleaved amplified polymorphic sequence (CAPS) marker and by detecting new Co/Ler polymorphisms in three YAC ends (CAPS marker for yUP5C8RE; RFLP markers for EG6C4LE and yUP17GLE; white boxes on the genetic map). (**B**) Sequences hybridizing to EST T20782 lie centrally in cosmid 23H12 and within pRSW1 [cloned into pBIN19 (*20*)]. The 14-exon *RSW1* gene produces a predicted protein product including transmembrane helices (hatched) and the D,D,D,QVLRW (*8*) signature. Conserved regions (black), variable regions (lighter), and residue numbers are based on the supplementary material (*17*). (**C**) Complementation of *rsw1*. T1 seeds of *rsw1* plants transformed (*21*) with cosmid 23H12 were selected for kanamycin resistance (21°C over 10 to 12 days). Two days at 31°C after 5 days at 21°C caused swelling of *rsw1* (left) but not of T2 (center) or wild-type (right) seedlings. (**D**) Wild-type (inset) and *rsw1* seedlings grown for 10 days at 31°C and viewed by cryoscanning electron microscopy. Epidermal cells in all organs of *rsw1* plants are misshapen.

trile. Shoots of *rsw1* seedlings grown at the restrictive temperature (31°C) have less cellulose than wild-type seedlings (159 ± 19 versus 363 ± 28 nmol of glucose per milligram of plant dry weight) but more of an ammonium oxalate–extracted glucan (195 versus 58 nmol mg^{-1}), which methylation analysis (Fig. 1A) and enzyme digestion show is β-1,4–linked (*4*). Facilitated extraction and digestion by enzymes and trifluoroacetic acid indicate low crystallinity, the property that makes cellulose resistant to extraction and digestion. Smaller changes in Golgi-synthesized polysaccharides show that *RSW1* is specifically involved in cellulose biosynthesis.

Rosettes (terminal complexes) are the putative hexameric cellulose synthase complexes of higher plant plasma membranes (*5*). Freeze-fractured root cells of wild type and mutant grown at 18°C show cellulose microfibrils (Fig. 1B). Rosettes on the P face of the mutant plasma membrane at 18°C (Fig. 1C) resemble those of the wild type, but transferring the mutant to 31°C reduces rosette numbers within 30 min, with extensive loss after 3 hours (Fig. 1D) and a loss of definition to the terminal globules on the E face. Plasma membrane particles tend to align in the mutant after prolonged exposure to the restrictive temperature (Fig. 1E). Cortical microtubules that align cellulose microfibrils and Golgi bodies that synthesize other wall polysaccharides appeared unchanged.

The *rsw1* mutation therefore disassembles cellulose synthase complexes, reduces cellulose accumulation, and causes β-1,4-glucan to accumulate in a noncrystalline form. It maps (*6*) to a region of chromosome 4 (Fig. 2A) to which a mapping program had assigned an expressed sequence tag (EST) that, it was deduced, might show weak similarities to a bacterial cellulose synthase (*7*). Full sequence of the EST partial cDNA indeed showed all except the first D of a D,D,D,QXXRW signature (*8*) characterizing a heterogeneous group of processive β-glycosyl transferases and more extended but still weak similarities to a subset (*9*). Correcting radial swelling by transforming *rsw1* (Fig. 2C) with full-length genomic clones (Fig. 2B) identical to sequences found on a yeast artificial chromosome (YAC) covering the mapped site proves that the gene is *RSW1*. The 3.8-kb *RSW1* transcript is widespread, as are misshapen cells in mutant plants grown at 31°C (Fig. 2D). A similarly sized transcript in the mutant is consistent with the mutant allele substituting Val for Ala^{549} after a C to T nucleotide change (*7*).

Four pieces of evidence make a compelling case that the *RSW1* gene product encodes the catalytic subunit of cellulose synthase: (i) The *rsw1* mutation selectively

```
MEASAGLVAGSYRRNELVRIRHESDGGTKPLKNMNGQICQICGDDVGLAETGDVFVACNECAFPVCRPCYEYERKDGTQCCPQCK  85
TRFRRHRGSPRVEGDEDEDDVDDIENEFNYAQGANKARHQRHGEEFSSSSRHESQPIPLLTHGHTVSGEIRTPDTQSVRTTSGPL 170
GPSDRNAISSPYIDPRQPVPVRIVDPSKDLNSYGLGNVDWKERVEGWKLKQEKNMLQMTGKYHEGKGGEIEGTGSNGEELQMADD 255
TRLPMSRVVPIPSSRLTPYRVVIILRLIILCFFLQYRTTHPVKNAYPLWLTSVICEIWFAFSWLLDQFPKWYPINRETYLDRLAI 340
RYDRDGEPSQLVPVDVFVSTVDPLKEPPLVTANTVLSILSVDYPVDKVACYVSDDGSAMLTFESLSETAEFAKKWVPFCKKFNIE 425
PRAPEFYFAQKIDYLKDKIQPSFVKERRAMKREYEEFKVRINALVAKAQKIPEEGWTMQDGTPWPGNNTRDHPGMIQVFLGHSGG 510
LDTDGNELPRLIYVSREKRPGFQHHKKAGAMNALIRVSAVLTNGAYLLNVDCDHYFNNSKAIKEAMCFMMDPAIGKKCCYVQFPQ 595
RFDGIDLHDRYANRNIVFFDINMKGLDGIQGPVYVGTGCCFNRQALYGYDPVLTEEDLEPNIIVKSCCGSRKKGKSSKKYNYEKR 680
RGINRSDSNAPLFNMEDIDEGFEGYDDERSILMSQRSVEKRFGQSPVFIAATFMEQGGIPPTTNPATLLKEAIHVISCGYEDKTE 765
WGKEIGWIYGSVTEDILTGFKMHARGWISIYCNPPRPAFKGSAPINLSDRLNQVLRWALGSIEILLSRHCPIWYGYHGRLRLLER 850
IAYINTIVYPITSIPLIAYCILPAFCLITDRFIIPEISNYASIWFILLFISIAVTGILELRWSGVSIEDWWRNEQFWVIGGTSAH 935
LFAVFQGLLKVLAGIDTNFTVTSKATDEDGDFAELYIFKWTALLIPPTTVLLVNLIGIVAGVSYAVNSGYQSWGPLFGKLFFALW 1020
VIAHLYPFLKGLLGRQNRTPTIVIVWSVLLASIFSLLWVRINPFVDANPNANNFNGKGGVF                          1081
```

Fig. 3. Sequence of the predicted *RSW1* gene product. The D,D,D,QXXRW signature is bold, conserved Cys residues are underlined, and Ala[549] (substituted with Val in *rsw1*) is bold and underlined.

inhibits cellulose synthesis and promotes accumulation of a noncrystalline β-1,4-glucan; (ii) *rsw1* disassembles plasma membrane rosettes, a plausible mechanism for reducing cellulose and placing the *RSW1* product in the rosettes or interacting with them; (iii) the D,D,D,QXXRW signature identifies the *RSW1* gene product as a processive glycosyl transferase (*9*) in family 2 of inverting nucleotide-diphospho-sugar glycosyltransferases (*10*) and with demonstrated uridine 5′-diphosphate–glucose binding ability in the highly similar cotton celA1 gene (*3*); and (iv) the wild-type allele corrects the mutant's radial swelling that results from reduced cellulose synthesis.

The deduced 122-kD *RSW1* product (Fig. 3) closely resembles the products of Ath-A and Ath-B [two full-length *Arabidopsis* cDNAs (*11*)], of the cotton celA genes proposed as cellulose synthase catalytic subunits (*3*), and of rice ESTs D48636 (*3*) and D39394 (*11*). Architecture is conserved (Fig. 2B): Six predicted membrane-spanning regions lie close to the COOH terminus, and two others separate an extended NH_2-terminal region from a central, probably cytoplasmic domain weakly similar to prokaryotic glycosyl transferases (*3*, *7*, *9*, *12*). Strikingly variable regions interrupt extended, highly conserved regions, which are particularly prominent in the central domain (*11*). The NH_2-terminal regions are heterogeneous except for a cysteine-rich domain that may cause protein-protein binding (*13*). The predicted products of five *Arabidopsis* genomic sequences (*14*) diverge further from *RSW1*, Ath-A, and Ath-B: they are smaller (710 to 828 amino acids versus 1081 in *RSW1*), lack an extended NH_2 terminus, vary in the number and position of predicted transmembrane helices, retain extensive sequence similarities in the central domain but have major insertions and deletions, and differ in their D,D,D spacings and QXXRW motifs. *Arabidopsis* EST fragments recently proposed as cellulose synthases (*15*) show little sequence similarity to *RSW1*. All belong to the large class of *Arabidopsis Csl* genes (cellulose-synthase–like) (*16*), but weak similarities do not prove a function in cellulose synthesis given the widely different polymers produced by enzymes sharing weakly related sequences (*10*). In our view, only Ath-A and Ath-B of the full-length *Arabidopsis* genes sufficiently resemble the functionally characterized *RSW1* to be prime candidates for additional cellulose synthases.

In conclusion, chemical and ultrastructural changes in the cellulose-deficient mutant combine with gene cloning, complementation of the mutant, and sequence analyses to show that the *RSW1* locus encodes the catalytic subunit of cellulose synthase. The noncrystalline β-1,4-glucan in the shoot of the *rsw1* mutant suggests that the mutant allele interrupts assembly of glucan chains into microfibrils. We hypothesize that at the restrictive temperature, mutant synthase complexes disassemble to monomers (or smaller oligomers) undetectable by freeze etching. The monomers continue producing β-1,4-glucan, but the dispersed chains fail to crystallize in an acid-resistant form. Crystallization—with consequences for wall mechanics that are central to morphogenesis and industrial fiber usage—therefore requires assembled rosettes.

REFERENCES AND NOTES

1. D. P. Delmer and Y. Amor, *Plant Cell* **7**, 987 (1995).
2. T. I. Baskin, A. S. Betzner, R. Hoggart, A. Cork, R. E. Williamson, *Aust. J. Plant Physiol.* **19**, 427 (1992).
3. J. R. Pear, Y. Kawagoe, W. E. Schreckengost, D. P. Delmer, D. M. Stalker, *Proc. Natl. Acad. Sci. U.S.A.* **93**, 12637 (1996).
4. Shoots from wild-type Columbia (Co) and backcrossed *rsw1* grown on agar for 7 days at 21°C or for 2 days at 21°C and 5 days at 31°C (*2*) were rinsed and stored in liquid nitrogen. Carbohydrate fractionation essentially as D. R. Heim, J. R. Skomp, C. Waldron, I. M. Larrinua, *Pestic. Biochem. Physiol.* **39**, 93 (1991). Glucan was extracted with ammonium oxalate from three separate batches of *rsw1*, purified in the supernatant after precipitation of pectins overnight with 2% cetyltrimethylammonium bromide. Glucose in trifluoroacetic acid hydrolysates was quantified against inositol internal standard by gas chromatography electron-impact–mass spectrometry (GC-MS) (Fisons MD800) of alditol acetates [S. H. Doares, P. Albersheim, A. G. Darvill, *Carbohydr. Res.* **210**, 311 (1991)]. Cellulose [acetic-nitric acid insoluble material; D. M. Updegraph, *Anal. Biochem.* **32**, 420 (1969)] was solubilized in 67% H_2SO_4, quantified by the anthrone-H_2SO_4 reaction, and contained ≥97% glucose by GC-MS. Methylation analysis [P. W. Needs and R. R. Selvendran, *Phytochem. Anal.* **4**, 210 (1993)] distinguished 1,3- and 1,4-linked material by retention time on a 12 mm by 0.22 mm (inner diameter) BPX 70 column (carrier He at 100 kPa, heated at 45°C for 5 min and raised to 220°C over 5 min) and by mass spectra [N. C. Carpita and E. M. Shea, in *Analysis of Carbohydrates by GLC and MS*, C. J. Biermann and G. D. McGinnis, Eds. (CRC Press, Boca Raton, FL, 1989), pp. 157–215]. The spectra of the partially methylated alditol acetates obtained from the glucan and cellulose were practically identical and contained peaks at mass/charge ratios *m/z* 117 and 233, corresponding to the most abundant primary fragments. The peak at *m/z* 161 was relatively small, and that at *m/z* 277 was barely visible. The spectra differed greatly from that of the partially methylated alditol acetate obtained from laminarin (a 1,3-linked glucan), in which the primary peaks at *m/z* 117, 161, and 233 were of comparable size and the peak at *m/z* 277 was significant. The close similarity of the mass spectra and elution times of the partially methylated alditol acetates demonstrates the presence of 1,4 rather than 1,3 linkages. Glucan produced by *rsw1* at 31°C (250 μg ml^{-1}) or starch (Sigma; 200 μg ml^{-1}) was digested with mixtures of endo-cellulase (E.C. 3.2.1.4; Megazyme, Australia) and β-glucosidase (E.C. 3.2.1.21; Sigma) or of α-amylase (E.C. 3.2.1.1; Sigma) and α-glucosidase (E.C. 3.2.1.20; Sigma). The former enzyme pair was inactive against 1,3-linked laminarin and starch but released 83% of the glucose released by trifluoroacetic acid from the *rsw1* glucan, whereas the latter pair released none but could release 95% of the glucose from starch.
5. W. Herth, in *Botanical Microscopy*, A. W. Robards, Ed. (Oxford Univ. Press, Oxford, 1985), pp. 285–310.
6. Visual mapping scored double mutant phenotypes in F2 plants [C. Koncz, N.-H. Chua, J. Schell, *Methods in* Arabidopsis *Research* (World Scientific, Singapore, 1992)] and showed linkage to *ga5*, whereas molecular mapping used RFLP [C. Chang, J. L. Bowman, A. W. Dejohn, E. S. Lander, E. M. Meyerowitz, *Proc. Natl. Acad. Sci. U.S.A.* **85**, 6856 (1988); H.-G. Nam *et al.*, *Plant Cell* **1**, 699 (1989)] or CAPS [A. Konieczny and F. Ausubel, *Plant J.* **4**, 403 (1993)] markers in F2 or F3 families from a cross to Landsberg (Ler). Mapping information at *Arabidopsis thaliana* Database (AtDB) (Stanford, CA).
7. EST T20782 became of interest when located to YACs in the *rsw1* interval as part of a mapping program [H. H. Höfte *et al.*, *Plant J.* **4**, 1051 (1993)] and aligned in a contig with four rice ESTs (D41986, D41766, D40691, and D41261) whose two 5′ members show weak sequence similarities to a bacterial cellulose synthase [H. C. Wong *et al.*, *Proc. Natl. Acad. Sci. U.S.A.* **87**, 8130 (1990); see supplementary material (*17*)]. DNA sequence analysis located the *RSW1* gene on genomic cosmid 23H12 [N. E. Olszewski, F. B. Martin, F. M. Ausubel, *Nucleic Acids Res.* **16**, 10765 (1988)], which hybridizes with the T20782 insert, and on YAC5C8, which spans the *rsw1* locus (Fig. 2A). T20782 is part of the *RSW1* transcript derived from exons 8 through 14 and 12 base pairs from exon 7. Exons 1 to 8 were sequenced from cDNA polymerase chain reaction (PCR) products amplified from Co double-stranded cDNA with primers upstream of the *RSW1* start site and a primer from within the EST. We determined the *rsw1* mutation by sequencing two PCR fragments spanning the full *rsw1* cDNA and *rsw1* genomic PCR fragments corresponding to the region.
8. Single-letter abbreviations for the amino acid residues are as follows: D, Asp; L, Leu; Q, Gln; R, Arg; V, Val; and W, Trp. X stands for any single residue; the commas stand for intervening sections of residues of arbitrary length.
9. For the D,D,D,QXXRW signature, see I. M. Saxena, R. M. Brown, M. Fevre, R. Geremi, B. Henrissat, *J. Bacteriol.* **177**, 1419 (1995). For sequences with similarities to the full EST, see A. G. Matthyse, S. White, R. Lightfoot, *ibid.*, p. 1069; H. J. Sofia, V. Burland, D. L. Daniels, G. Plunkett III, F. R. Blattner, *Nucleic Acids Res.* **22**, 2576 (1994).
10. J. A. Campbell, G. J. Davies, V. Bulone, B. Henrissat, *Biochem. J.* **326**, 929 (1997).
11. Ath-A and Ath-B were cDNA clones isolated by hy-

bridization from a cDNA library of 21-day-old Co plants using a PCR fragment spanning the 5′ part of *RSW1* transcript. Ath-A is on YAC CIC9H6, chromosome 4. The EST T20782 clone was from *Arabidopsis* Biological Resource Center (Columbus, OH); rice EST D39394, from the MAFF DNA Bank (Tsukuba, Japan). The sequences were analyzed at the Australian National Genome Information Service with the use of Wisconsin GCG software [J. Devereux, P. Haeberley, O. Smithies, *Nucleic Acids Res.* **12**, 387 (1984)]. Sequences for *RSW1*, Ath-A, Ath-B, and rice D39394 have been deposited at GenBank (AF027172, AF027173, AF027174, and AF030052, respectively); comparisons are provided as supplementary material (*17*).
12. I. M. Saxena, F. C. Lin, R. M. Brown, *Plant Mol. Biol.* **15**, 673 (1990); G. F. Kutish *et al.*, *Virology* **223**, 303 (1996).
13. The first 90 residues of the predicted gene products of *RSW1*, Ath-A, Ath-B, rice EST D39394, and cotton celA1 resemble three putative plant basic leucine zipper transcription factors (X97904, L28003, and L28004) with conserved Cys spacing (underlined, Fig. 3). Similar motifs are implicated in protein-protein or protein-lipid interaction [P. S. Freemont, *Ann. N.Y. Acad. Sci.* **684**, 174 (1993)], and celA1 was reported to bind Zn^{2+} [Y. Kawagoe and D. P. Delmer, *Plant Physiol.* **114** (suppl.), 85 (1997)].
14. Five protein sequences (accession numbers 2262116, 2262115, 2262114, 2244887, and 2244890) were identified by Gapped BLASTX searches of GenBank with the use of RSW1 and were analyzed as in (*11*).
15. I. M. Saxena and R. M. Brown, *Cellulose* **4**, 33 (1997).
16. S. Cutler and C. Somerville, *Curr. Biol.* **7**, R108 (1997).
17. Supplementary material available at www.sciencemag.org/feature/data/974564.shl
18. W. Herth, *Planta* **164**, 12 (1985); B. Schneider and W. Herth, *Protoplasma* **131**, 142 (1986).
19. R. Schmidt, J. West, G. Cnops, A. Balestrazzi, C. Dean, *Plant J.* **9**, 755 (1996).
20. M. Bevan, *Nucleic Acids Res.* **12**, 8711 (1984).
21. N. Bechtold, J. Ellis, G. Pelletier, *C. R. Acad. Sci. Paris* **316**, 1194 (1993).
22. We thank R. Schmidt and C. Lister for sharing mapping information and clones. Supported by the Australian National University (A.C., J.P., L.P., J.R., and R.E.W.), Australian Research Council (J.P.), Cooperative Research Centre for Plant Science (T.A., R.B., A.C., J.B., and L.P.), Cotton Seed Distributors (T.A. and J.G.), Deutsche Forschungsgemeinschaft (A.S.B., W.H., and W.W.), Groupe Limagrain Pacific (A.S.B.), Groupement de Recherches et d'Etudes sur les Génomes and Actions Coordonnées Concertées dans le Domaine des Sciences du Vivant (C.C. and H.H.), and North Eucalypt Technologies (J.B. and J.G.).

20 August 1997; accepted 18 December 1997

Alopecia Universalis Associated with a Mutation in the Human *hairless* Gene

Wasim Ahmad, Muhammad Faiyaz ul Haque, Valeria Brancolini, Hui C. Tsou, Sayed ul Haque, HaMut Lam, Vincent M. Aita, Jason Owen, Michelle deBlaquiere, Jorge Frank, Peter B. Cserhalmi-Friedman, Andrew Leask, John A. McGrath, Monica Peacocke, Mahmud Ahmad, Jurg Ott, Angela M. Christiano*

There are several forms of hereditary human hair loss, known collectively as alopecias, the molecular bases of which are entirely unknown. A kindred with a rare, recessively inherited type of alopecia universalis was used to search for a locus by homozygosity mapping, and linkage was established in a 6-centimorgan interval on chromosome 8p12 (the logarithm of the odds favoring linkage score was 6.19). The human homolog of a murine gene, *hairless*, was localized in this interval by radiation hybrid mapping, and a missense mutation was found in affected individuals. Human *hairless* encodes a putative single zinc finger transcription factor protein with restricted expression in the brain and skin.

The human hair follicle is a dynamic structure that generates hair through a complex and exquisitely regulated cycle of growth and remodeling (*1*). Despite the extensive descriptive understanding of the hair cycle, currently, very little is known about the molecular control of the signals that regulate progression through the hair cycle, although it is clear that at least some potentially influential regulatory molecules may play a role (*1*). For example, a knock-out mouse with targeted ablation of the gene encoding the fibroblast growth factor 5 (FGF5) provided evidence that FGF5 is an inhibitor of hair elongation, and the mouse had an increase in hair length due to an increase in the time that follicles remain in anagen. The FGF5 gene was also deleted in the naturally occurring mouse model, *angora* (*2*). Another member of the FGF family, FGF7 or keratinocyte growth factor, was disrupted by gene targeting, and the resultant mouse had hair with a greasy, matted appearance, similar in phenotype to the *rough* mouse (*3*). A transgenic mouse was engineered that disrupted the spatial and temporal expression of the gene encoding the lymphoid enhancer factor 1, a transcription factor that binds to the promoter region of several published hair keratin promoters. Disruption of this potential master regulator of hair keratin transcription resulted in defects in the positioning and angling of the hair follicles (*4*). More recently, a mutation in a structural protein, mouse desmoglein 3 (encoded by the gene *dsg3*), was found to be the underlying mutation in the naturally occurring mouse phenotype, *balding* (*5*). Finally, the *nude* mouse phenotype, characterized by hairlessness and athymia, was found to be the result of mutations in the winged-helix *nude* (*whn*) gene, a member of the winged-helix class of transcription factors (*6*). In addition to the complexity of the signaling pathways, in sheep, there are over 100 distinct structural proteins synthesized by the hair cortex and cuticle cells that produce the keratinized structure of a wool fiber (*1*). Despite these examples of recent progress in animal models, we have only begun to understand the control and molecular complexity of the hair follicle and its cyclic progression in humans.

There are several forms of hereditary human hair loss, known collectively as alopecias, which may represent a dysregulation of the cycle of hair growth and remodeling (*1*), yet the molecular basis of the alopecias has remained largely unexplored (*7*). The most common form of hair loss, known as androgenetic alopecia (male pattern baldness), is believed by some to affect ~80% of the population (*7*). Alopecia areata is a common dermatologic disease affecting about 2.5 million individuals in the United States alone, which causes round, patchy hair loss on the scalp (*7*). Alopecia areata can progress to involve hair loss from the entire scalp; this condition is referred to as alopecia totalis. Alopecia universalis (AU) is the term for the most extreme example of disease progression, which results in the complete absence of scalp and body hair (*7*). Although an autoimmune pathomechanism for alopecia areata has been

W. Ahmad, H. C. Tsou, H. Lam, V. M. Aita, J. Frank, P. B. Cserhalmi-Friedman, M. Peacocke, A. M. Christiano, Department of Dermatology and Department of Genetics and Development, Columbia University, 630 West 168 Street, VC-15-526, New York, NY 10032, USA.
M. F. ul Haque, S. ul Haque, M. Ahmad, Department of Biological Sciences, Quaid-i-Azam University, Islamabad, Pakistan.
V. Brancolini and J. Ott, Laboratory for Statistical Genetics, Rockefeller University, 1230 York Avenue, New York, NY 10021, USA.
J. Owen and M. deBlaquiere, Research Genetics, Inc., 2130 Memorial Parkway SW, Huntsville, AL 35801, USA.
A. Leask, FibroGen, Inc., 260 Littlefield Avenue, South San Francisco, CA 94080, USA.
J. A. McGrath, St. John's Institute of Dermatology, St. Thomas' Hospital, Lambeth Palace Road, London, SE1 7EH, UK.

*To whom correspondence should be addressed. E-mail: amc65@columbia.edu